THE ASTROPHYSICAL JOURNAL, 464:476–486, 1996 June 10

THE INFLUENCE OF MAGNETISM ON *p*-MODE SURFACE AMPLITUDES

REKHA JAIN, BRADLEY W. HINDMAN, AND ELLEN G. ZWEIBEL
JILA, NIST and University of Colorado, Campus Box 440, Boulder, CO 80309;
rjain@suraj.colorado.edu; hindman@solarz.colorado.edu; zweibel@lepton.colorado.edu
Received 1995 August 31; accepted 1995 December 19

ABSTRACT

We propose a mechanism to explain the observed suppression of *p*-mode surface velocities in solar active regions. We show that a horizontal magnetic field can lower the upper turning point and change the skin depth for a simple plane-parallel adiabatically stratified polytrope. In addition to power suppression, the magnetic field alters the phase of *p*-modes. Simultaneous measurements of *phase* as well as *amplitude* in the active and quiet regions would provide an additional diagnostic for probing the structure of active region magnetic fields.

Subject headings: Sun: activity — Sun: magnetic fields — Sun: oscillations

1. INTRODUCTION

Observations show that *p*-mode power is substantially suppressed in magnetic regions (see Lites, White, & Packman 1982; Tarbell et al. 1988; Title et al. 1992). The reduction in power in magnetic regions can be large as a factor of 2–3 relative to nonmagnetic regions (Tarbell et al. 1988). Cally (1995) investigated the effects of weak-to-moderate vertical magnetic fields on solar *f*- and *p*-modes and suggests "slow mode leakage" as a responsible mechanism. According to this mechanism, the slow magnetoacoustic wave propagates out of the acoustic cavity carrying away *p*-mode energy from layers close to the surface. Another possible explanation is that the upper turning point (acoustic cutoff point) of the solar *p*-modes is lowered in the presence of a magnetic field (Title et al. 1992; Brown 1994). A related possibility is the the attenuation length or skin depth in the evanescent region is reduced in the presence of a magnetic field. Furthermore, it is likely that the observations sample a different position in the evanescent tail of the *p*-mode eigenfunction in magnetic regions because of magnetic effects on the temperature structure of the atmosphere.

In this paper, we use a simple model to illustrate some aspects of these effects. We discuss how the presence of horizontal magnetic fields affects the acoustic cutoff point and the surface amplitude of the *p*-mode eigenfunctions and present qualitative results that clearly show that magnetism can play an important role in the apparent suppression of *p*-mode power. We also take up the question of whether the reduction of power carries any information about the structure of the solar magnetic field, which might thus lead to diagnostics.

Briefly summarized, our findings are as follows. Horizontal magnetic fields can cause suppression of *p*-mode amplitudes, but not under all conditions; the effect depends upon the run of magnetic field with depth. Magnetic fields can in principle be distinguished from acoustic perturbations, but only by effects depending on the direction of propagation. The effect of the magnetic field on the acoustic cutoff point, which is independent of propagation angle, can always be duplicated by a perturbation to the sound speed.

The paper is organized as follows. In § 2, we present a description of the generalized governing equations and how they reduce for the model in consideration. Section 3 deals with various results regarding the upper turning point and skin depth. In § 4, we discuss, on the basis of our present simple model, the effects of the magnetic fields on the solar *p*-modes.

2. THE GOVERNING EQUATIONS

Consider a perfectly conducting ideal gas permeated by a horizontal magnetic field $\boldsymbol{B} = B(z)\hat{\boldsymbol{x}}$. The equilibrium state is described by the equations:

$$\frac{d}{dz}\left(p + \frac{B^2}{8\pi}\right) = -\rho(z)g\,, \tag{1}$$

$$p = \mathscr{R}\rho T\,, \tag{2}$$

where $p(z)$, $\rho(z)$, and $T(z)$ are the gas pressure, density, and temperature, respectively. Gravity acts in the negative z-direction and is assumed to be constant; the gas constant $\mathscr{R}$ is $k_B/\hat{m}_p$, where k_B is Boltzmann's constant and $\hat{m}_p$ is the mean molecular weight.

We restrict ourselves in this paper to purely vertical (or radial) displacements $\boldsymbol{v} = (0, 0, v_z)$ about the equilibrium (eqs. [1] and [2]). This case captures the effect of the magnetic field on the acoustic cutoff frequency. This is the dominant magnetic effect on *p*-modes as long as the magnitude k_h of the horizontal wavenumber $\boldsymbol{k}_h$ and characteristic scale heights H satisfy the inequality $k_h H \ll 1$. At sufficiently short wavelengths, terms proportional to $k_h^2 B^2$, which represent the restoring forces of magnetic pressure and tension, become important. These terms depend on the relative angle between $\boldsymbol{k}_h$ and $\boldsymbol{B}$ and as such carry information about the direction of the magnetic field. The value of k_h at which these Lorentz force terms become important may be roughly estimated as ω_{ac}/c_s, where ω_{ac} and c_s are the acoustic cutoff frequency and sound speed, respectively. For photospheric values of the parameters the corresponding l value for the mode must be of order 3000; at lower values of l, cutoff effects dominate and the approximation made in this paper should be reasonably accurate. We have written down some of these terms elsewhere (Jain, Hindman, & Zweibel 1995) and will return to the wavenumber-dependent effects in a future paper (Hindman, Jain, & Zweibel 1996).

According to the linearized MHD equations of ideal MHD (see, e.g., Thomas 1983), the vertical component of

the velocity $v_z(z)\exp i\omega t$ is governed by the equation

$$\mathscr{A}_1\frac{d^2v_z}{dz^2}+\mathscr{A}_2\frac{dv_z}{dz}+\mathscr{A}_3 v_z=0\,, \tag{3}$$

where

$$\mathscr{A}_1=c_s^2+v_A^2\,,\quad \mathscr{A}_2=\rho^{-1}\frac{d}{dz}\left[\rho(c_s^2+v_A^2)\right]\,,\quad \mathscr{A}_3=\omega^2\,. \tag{4}$$

Here, γ is the adiabatic exponent (taken to be constant); $c_s(z)=(\gamma p/\rho)^{1/2}$ is the adiabatic sound speed and $v_A(z)=\{B^2/[4\pi\rho(z)]\}^{1/2}$ is the Alfvén speed. Notice that the Alfvén and sound speeds appear on exactly the same footing. This means that it is impossible to distinguish magnetic effects from acoustic effects in the limit $k_h\to 0$ if the density profile is the same in the magnetic and nonmagnetic models.

We reduce equation (3) to a canonical form through the substitution

$$v_z=V(z)P(z) \tag{5}$$

where $V(z)$ is governed by the canonical equation

$$\frac{d^2V}{dz^2}+\kappa^2V=0;\quad \kappa^2=\frac{\mathscr{A}_3}{\mathscr{A}_1}-\frac{1}{2}\frac{d}{dz}\left(\frac{\mathscr{A}_2}{\mathscr{A}_1}\right)-\frac{\mathscr{A}_2^2}{4\mathscr{A}_1^2}\,, \tag{6}$$

and

$$P(z)=\exp\left(-\frac{1}{2}\int\frac{\mathscr{A}_2}{\mathscr{A}_1}\,dz\right). \tag{7}$$

The wavenumber κ^2 can be written as

$$\kappa^2=\frac{\omega^2-\omega_{\rm mac}^2}{[c_s^2(z)+v_A^2(z)]}\,, \tag{8}$$

where the magnetoacoustic cutoff frequency $\omega_{\rm mac}^2$ is defined by

$$\omega_{\rm mac}^2\equiv\frac{[\gamma g+(2-\gamma)(V_A^2/H_m)]^2}{4(c_s^2+v_A^2)}+\frac{\gamma g+(2-\gamma)(v_A^2/H_m)}{2(c_s^2+v_A^2)}\times\frac{d}{dz}(c_s^2+v_A^2)-\frac{(2-\gamma)}{2}\frac{d}{dz}\left(\frac{v_A^2}{H_m}\right), \tag{9}$$

and the magnetic scale height by $H_m^{-1}\equiv-(1/B)(dB/dz)$. Note that $\omega_{\rm mac}^2$ is quite different from the nonmagnetic acoustic cutoff frequency, $\omega_{\rm ac}^2$, which is given by

$$\omega_{\rm ac}^2\equiv\frac{\gamma^2g^2}{4c_s^2(z)}+\frac{\gamma g}{2c_s^2(z)}\frac{dc_s^2}{dz}\,. \tag{10}$$

However, if the adiabatic index γ of the gas happens to be equal to 2, which is the "adiabatic index" for one-dimensional compression of a magnetic field, equation (9) would be the same as equation (10) with the magnetoacoustic speed $(c_s^2+v_A^2)^{1/2}$ replacing the acoustic speed. This shows that the somewhat complicated form of $\omega_{\rm mac}$ is caused by the differing compressibilities of the thermal and magnetic gases. Also note that these are the cutoff frequencies for v_z and not for $\nabla\cdot\boldsymbol{v}$; in general these are not the same (see, e.g., Gough, 1991).

In § 3 we compute turning points and eigenfunctions for p-modes in four simple model atmospheres. All of these atmospheres are based on a polytrope modified by magnetic fields. For the polytrope, the temperature $T(z)$ varies linearly with depth:

$$T(z)=T_0\left(1-\frac{z}{z_0}\right),\quad z<z_0\,; \tag{11}$$

T_0 is the temperature at the reference level $z=0$ and $z=z_0>0$ is the surface. The equilibrium density and pressure can be calculated using equations (1) and (2):

$$\rho(z)=\frac{p_0}{\mathscr{R}T_0}\left(1-\frac{z}{z_0}\right)^m,\quad z<z_0\,; \tag{12}$$

$$P(z)=p_0\left(1-\frac{z}{z_0}\right)^{m+1},\quad z<z_0\,; \tag{13}$$

where $m=(gz_0/\mathscr{R}T_0)-1$ is the polytropic index and p_0 is the gas pressure at $z=0$. For a "convectively neutral" atmosphere with zero buoyancy, $m=1/(\gamma-1)$. This is the case considered here. The quantity z_0 introduced in equation (11) can now be identified as $z_0=(m+1)\mathscr{R}T_0/g$. The acoustic cutoff frequency for this atmosphere is $\omega_{\rm ac}^2=\gamma(2-\gamma)g^2/4c_s^2$, which diverges at the surface $z=z_0$.

In the absence of magnetic field, equations (1), (11), and (12) reduce the governing equation (3) to

$$\frac{d^2v_z}{dz^2}-\frac{(m+1)}{(z_0-z)}\frac{dv_z}{dz}+\frac{m\omega^2}{g(z_0-z)}v_z=0\,. \tag{14}$$

In order that v_z and dv_z/dz are bounded at the surface $z=z_0$, the solution of equation (14) is given by (see Abramowitz & Stegun 1970)

$$v_z=\mathscr{C}(z_0-z)^{-(m/2)}J_m\left[2\omega\sqrt{\frac{m}{g}(z_0-z)}\right], \tag{15}$$

where $\mathscr{C}$ is an arbitrary constant and J_m is the Bessel function of the first kind. Note that, according to equation (15), these horizontally invariant oscillations are not quantized in frequency. The lack of quantization is a consequence of our use of slab geometry rather than spherical geometry and the discrepancy with solar oscillations is not important for the purpose of this paper.

3. RESULTS

All of the numerical examples shown in the figures use the set of parameters $T_0=4200$ K, $p_0=868.2$ ergs cm^{-3}, $\gamma=5/3$, $m=1.5$, $\mathscr{R}=6.425\times10^7$ cm^2 s^{-2} K^{-1}, and $g=2.74\times10^4$ cm s^{-2}. The values are taken from the Harvard-Smithsonian Reference Atmosphere and correspond to those at the temperature minimum (see Gingerich et al. 1971). The sound speed is 6.7 km s^{-1} at the reference height ($z=0$). The cyclic frequency is denoted by ν.

3.1. *Upper Turning Point*

We consider four different simple magnetic field profiles.

Case 1: Uniform B[$B(z)=B_0$].—The magnetic field is considered to be uniform, and the field strength is assumed to be $B_0=200$ G, corresponding to an Alfvén speed of $\sim$9.95 km s^{-1} at the reference height. In the case of uniform fields, the equilibrium pressure, density, and hence the sound speed, $c_s(z)$ remain unchanged from the nonmagnetized model. Thus the temperature, density, and pressure profiles are given by equations (11), (12), and (13). It is evident from Figure 1 that the upper turning point is

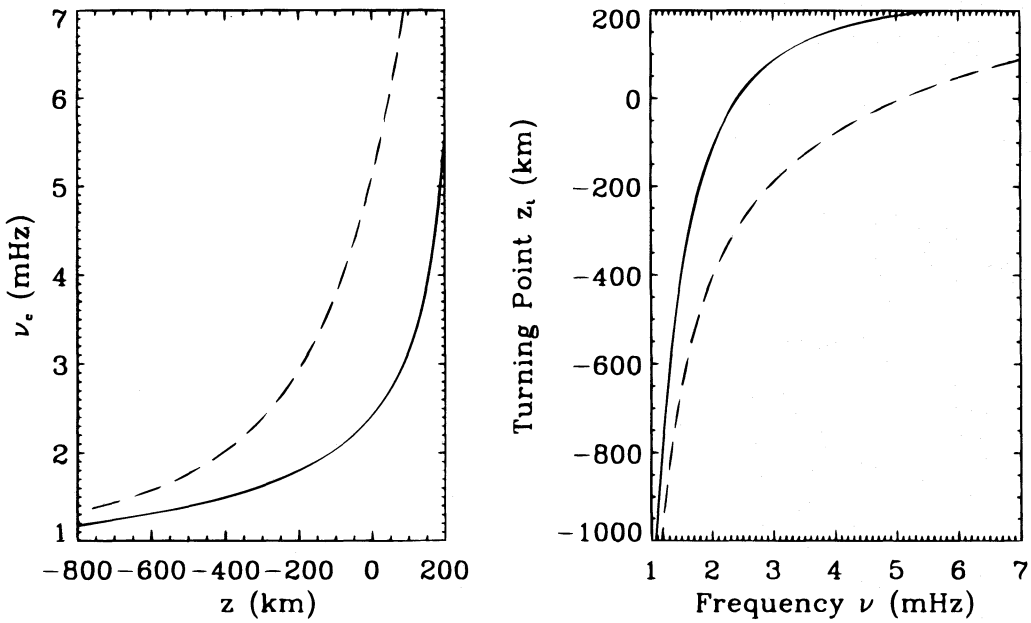

FIG. 1.—The cutoff frequency ν_c (*left*) (in mHz) as a function of z (*right*) (in kilometers) for the uniform B case. Solid curves are for the nonmagnetized model (i.e., acoustic cutoff frequency), and the dashed curves for the magnetized model (i.e., magnetoacoustic cutoff frequency). Note the increase in cutoff frequencies and the decrease in the upper turning points (*dashed curves*) in the presence of such a field. Also note that this is frequency dependent.

lowered in the presence of such a field. This occurs because of the large increase in Alfvén speed toward the surface $z = z_0$, which creates a magnetoacoustic barrier of modest size.

Case 2: Uniform v_A.—In this case we consider the equilibrium magnetic field $B(z)$ and density $\rho(z)$, to be structured in such a way that $B^2(z) \propto \rho(z)$, so that the Alfvén speed is constant. We consider the example where $v_A \approx 7.5$ km s^{-1} throughout the polytrope. We also assume that the magnetic field does not modify the sound speed as a function of depth. Thus, the temperature profile is given by equation (11), and one may obtain the following expression for the density.

$$\rho(z) = \frac{p_0}{\mathcal{R}T_0}\left[\frac{\gamma v_A^2 + 2c_s^2(z)}{2c_0^2}\right]^m; \quad c_0^2 \equiv \frac{\gamma g z_0}{(m+1)}. \tag{16}$$

This way, the density in the magnetized and nonmagnetized model is the same at depth but unlike the nonmagnetized model, the density here is not zero at the surface. It is clear from Figure 2 that, unlike the uniform B case, the acoustic cutoff frequencies decrease in the presence of such a field. We can understand this behavior as follows. Near the top of the atmosphere, v_A dominates c_s, and it can be shown that $\omega_{mac}^2 \propto g^2/v_A^2$, so the magnetoacoustic barrier is lower than the purely acoustic barrier. At large depths $c_s \gg v_A$, and it can be shown that

$$\omega_{mac}^2 \approx \omega_{ac}^2\left[1 - \frac{v_A^2}{c_s^2}\left(5 - \frac{4}{\gamma}\right)\right], \tag{17}$$

so the barrier is lowered by a factor of order $(1 - v_A^2/c_s^2)$. At intermediate depths the cutoff frequency is also lowered.

Case 3: Gaussian profile for $B^2(z)$: same densities.—We now consider $B^2(z) = B_0^2 e^{[-(z+z_d)/a]^2}$. Relevant quantities are illustrated in Figure 3 is for the case $B_0 = 200$ G, $z_d = 300$ km and $a = 100$ km. In this case we assume that the density $\rho(z)$ remains unchanged between the nonmagnetized and the magnetized model and is given by equation (12). The pressure $p(z)$ in the presence of such a field is then given by

$$p(z) = p_0\left(1 - \frac{z}{z_0}\right)^{m+1} + \frac{B^2(z_0)}{2\mu} - \frac{B^2(z)}{2\mu}. \tag{18}$$

It is clear that the temperature profile (sound speed) must change (see Fig. 3) so as to keep the layer cooler. The magnetoacoustic speed $(c_s^2 + v_A^2)^{1/2}$, however, exceeds by a small amount the acoustic speed in the unmagnetized reference model. This is generally the case in a neutrally buoyant magnetic layer, because the magnetic field has $\gamma = 2$, a larger value of γ than the thermal pressure it replaces. It can be shown from equation (9) that for such a localized magnetic field the first term is always positive, but since $(d/d_z)(v_A^2/H_m) > 0$ between ≈ -200 km and ≈ -400 km, the third term is negative in this layer. The combination of v_A^2/H_m and $(d/d_z)(c_s^2 + v_A^2)$ makes the second term also negative between ≈ -200 km and ≈ -400 km. Thus, we expect ω_{mac}^2 to be negative in the region where the magnetic field is strong. Since the sound speed and Alfvén speed profiles are symmetrical about $z = -300$ km, the changes in the magnetoacoustic cutoff frequency ν_{mac} are also expected to be fairly symmetrical. Note that in Jain et al. (1995), the magnetoacoustic cutoff frequency was plotted incorrectly. The corrected version is shown here in Figure 3.

Although the large gradients associated with a thin magnetic layer cause large local increases in the cutoff frequency, the associated acoustic barrier is geometrically thin, so waves can tunnel through them with little attenuation. The attendant mode suppression is therefore expected to be small.

Figure 3 also shows, as expected, that only modes with upper turning points within the layer can be affected by it. This shows that selective reduction of mode power could be a diagnostic of localized, subsurface perturbations.

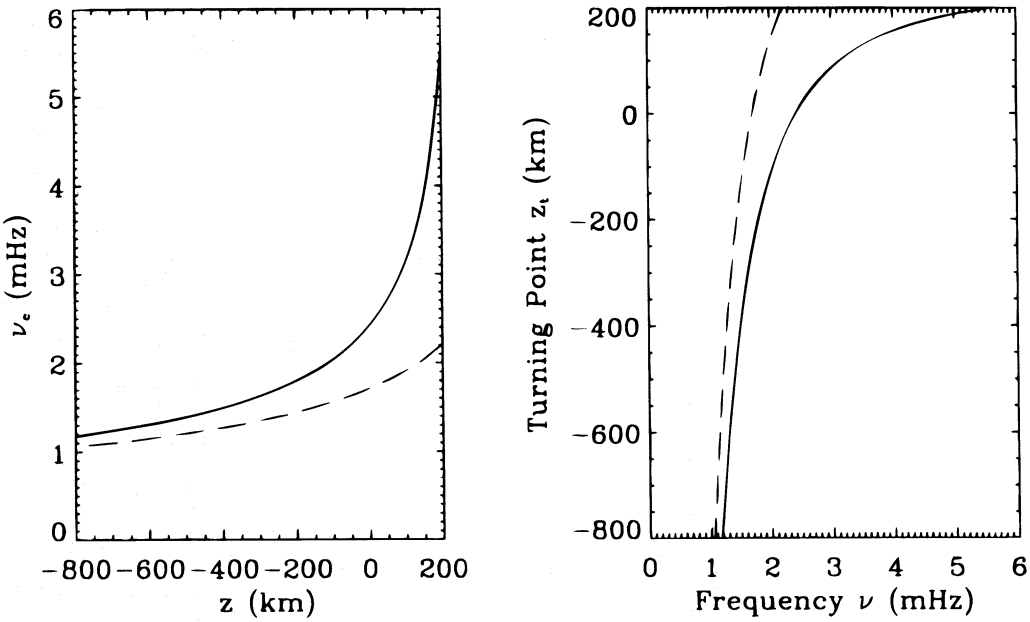

FIG. 2.—The cutoff frequency v_c (*left*) as a function of z (*right*) for uniform v_A case. Note the decrease in cutoff frequencies (*dashed curves*) in the presence of such a magnetic field.

The three cases considered here show strikingly different behavior in the size and even the sign of the effect and its dependence on frequency (or, more generally, lower turning point). What effects have been omitted from these models, and which, if any, corresponds to generally accepted ideas about the structure of the solar magnetic field? In answer to the first question, we have not accounted for the possible fibril nature of the field, which would probably increase the size of the effect, just as concentrating magnetic flux into bundles increases its effect on mode frequencies (Bogdan & Zweibel 1985), nor have we accounted for possible variations in heating associated with the magnetic field. As for the second question, it seems unlikely that the field increases with depth as fast as $\rho^{1/2}$ (second model), as this would imply very large fields even at moderate depths. The third model, the thin layer of magnetic field, is locally unstably stratified (Newcomb 1961), and the choice of density is not justified thermodynamically. These problems reflect the well-known difficulty of storing magnetic flux tubes in the solar convection zone. It is thus important to construct a neutrally stable atmosphere with localized magnetic field, which solves the stability although not the thermodynamic problem. The next case takes this point into account.

Case 4: Neutrally stable model with localized magnetic fields.—From hydrostatic equilibrium equation, we have

$$\frac{dp}{dz} + g\rho = -\frac{dp_m}{dz}, \tag{19}$$

where $p_m = [B^2(z)]/2\mu$, is the magnetic pressure. Introducing marginal stability into the hydrostatic equation yields the Brunt-Väisala frequency in the presence of a magnetic field:

$$N_B^2 = \frac{g}{\gamma p}\left(g\rho + \frac{dp_m}{dz}\right) + \frac{g}{\rho}\frac{d\rho}{dz}. \tag{20}$$

Assuming $N_B^2 = 0$, i.e., enforcing the marginal stability condition $(d\rho/dz) = (\rho/\gamma p)(dp/dz)$ in equation (19), yields

$$\frac{dc_s^2}{dz} + (\gamma - 1)g = -\frac{(\gamma - 1}{\rho}\frac{dp_m}{dz}. \tag{21}$$

By specifying the plasma $\beta \equiv p/p_m$, we can solve equations (19) and (21) for p and c_s^2, respectively. As an example, we choose β to be

$$\beta(z) = \beta_0 \exp\left[\left(\frac{z + z_d}{a}\right)^2\right]. \tag{22}$$

In Figure 4, we have taken $\beta_0 = 0.3$, $z_d = 300$ km and $a = 100$ km. This then corresponds to a magnetic field strength of $\approx$415 G at $z = -300$ km. The buoyancy frequencies are zero for both the magnetized and unmagnetized atmospheres. We solve equations (19) and (21) by imposing the boundary condition that at $z \to -\infty$, the gas pressure and the sound speed are the same in the nonmagnetized and magnetized models. Note that the magnetized atmosphere is not polytropic around $z = -300$ km because of the localized magnetic field. Also note that the surface of the magnetized atmosphere has moved further out (see Fig. 4*c*). In other words, the atmosphere has puffed up near the surface. This can be understood as a mass conservation effect. By Bernoulli's integral, the pressure at depth supports the overlying weight and is the same in the magnetized and unmagnetized models. The magnetized region is partially evacuated, so there must be a density enhancement above the magnetic layer.

In Figure 4*d*, we have plotted the magnetoacoustic cutoff frequency as a function of z for this model. The result is similar to the Gaussian case shown in Figure 3*c*. What drives $v_{\rm mac}^2$ to be negative can be understood as follows. Refer to equation (9). It is clear that $(c_s^2 + v_A^2)$ is positive throughout, so the first term in the equation (9) is always positive. However, the second term becomes negative

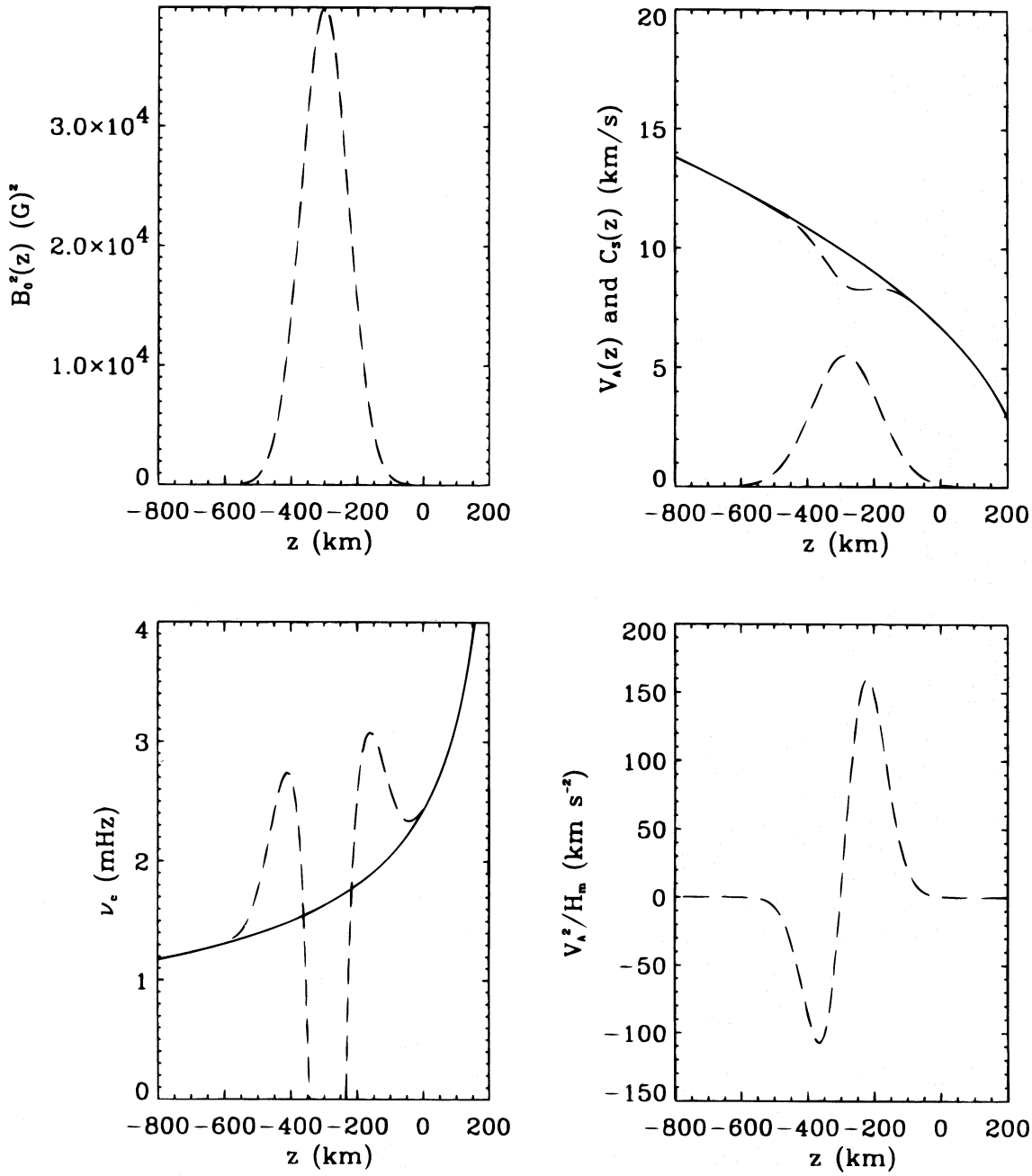

FIG. 3.—Various parameters like (*a*) the magnetic pressure, (*b*) the Alfvén and sound speeds, (*c*) the cutoff frequency ν_c, and (*d*) v_A^2/H_m as a function of z for a Gaussian profile for $B^2(z)$. Note that the square of the magnetoacoustic cutoff frequencies (*dashed curves*) is negative in the presence of such a field.

between −150 km and −360 km due to the combined effect of v_A^2/H_m and $(d/dz)(c_s^2 + v_A^2)$. When $(d/dz)(c_s^2 + v_A^2) < 0$, $v_A^2/H_m > 0$ and vice versa, thus maintaining a negative sign for the second term in this region. Also, $(d/dz)(v_A^2/H_m) > 0$ in this region and hence the third term is negative. It is the combination of second and third terms, which dominates the first term, in equation (9) leading to a negative v_{mac}^2. Figure 4*d* shows an impressively large magnetoacoustic barrier just below the magnetic layer. However, the barrier is geometrically so thin that most modes tunnel through it will little attenuation—likewise for the second, smaller barrier that occurs just above the layer. Thus, little power suppression is expected.

3.2. *Eigenfunctions*

We expect changes to the eigenfunctions v_z in the presence of a magnetic field in addition to the change in turning point. The magnitude of the effect should depend upon the structure of the magnetic atmosphere and the frequency of the mode. We consider a few examples to illustrate this. The eigenfunction for the nonmagnetized model is calculated using equation (15). We solve equation (3) numerically, for a uniform field strength $B = 200$ G, where the coefficients $\mathscr{A}_1$, $\mathscr{A}_2$, and $\mathscr{A}_3$ are given by equation (4). (The WKB approximation is violated near the turning point and in fact in a significant part of the domain. Therefore we choose to solve

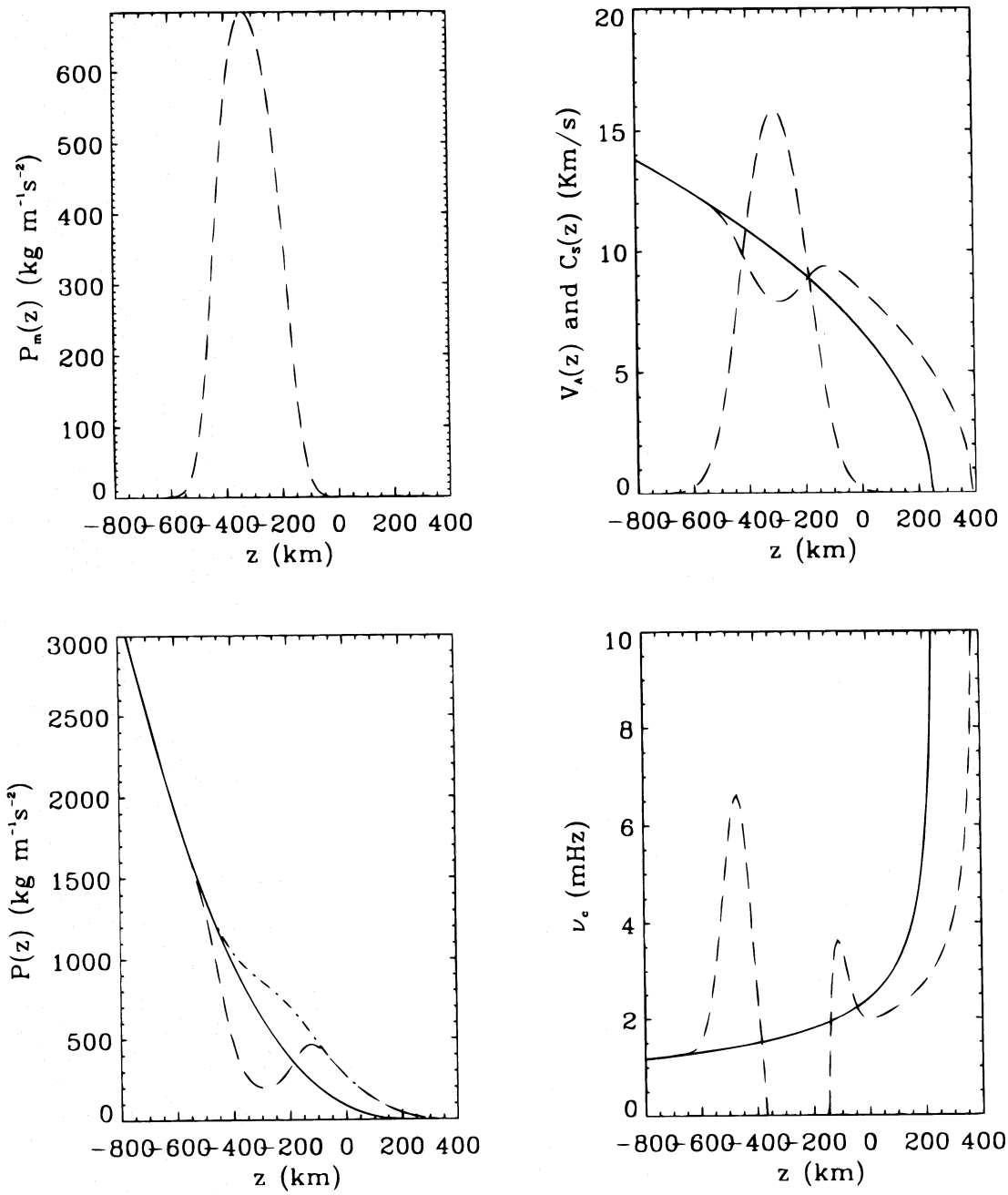

FIG. 4.—Various parameters like (*a*) the magnetic pressure, (*b*) the Alfvén and sound speeds, (*c*) the gas pressure, and (*d*) the cutoff frequencies as a function of z for neutrally stable atmosphere (case 4). The dashed curves represent the parameters in the magnetized model whereas the solid curves are for nonmagnetic polytrope model. The dot-dashed line in the pressure diagram is the total (gas + magnetic) pressure in the magnetized model.

the wave equation itself rather than using the WKB approximation). We impose the boundary conditions that (*a*) the amplitudes are the same deep in the nonmagnetized and magnetized atmospheres and (*b*) the Lagrangian pressure perturbation at the surface is zero.

Consider a mode of frequency $\nu = 2$ mHz. Note from Figure 1 that a mode of frequency 2 mHz has an upper turning point at around $z = -100$ km in the absence of magnetic field and at around $z = -400$ km in the presence of a uniform 200 G field.

Figure 5 compares the eigenfunctions v_z as a function of z for the nonmagnetized and magnetized models (case 1). The solid curve represents the solution in the nonmagnetized model. The solution is generated by using equation (15) since it gives finite dv_z/dz at the surface. The dashed curve corresponds to the eigenfunction in the presence of a uniform 200 G field. The solution, in general, is given by $v_z(z) = \mathscr{A}T_j(z) + \mathscr{B}T_y(z)$ where T_j and T_y asymptotically approach the J and Y Bessel function solutions of equation (14) as $z \to -\infty$. The coefficients $\mathscr{A}$ and $\mathscr{B}$ are then determined by the two boundary conditions, and equation (3) is integrated once again with the known values of $\mathscr{A}$ and $\mathscr{B}$. This way, the amplitude of the waves are the same as in the unmagnetized case at $z \to -\infty$ and $dv_z/dz = 0$ at $z = z_0$. It is clear from Figure 5*a* that the eigenfunctions are the same for both cases throughout the polytrope except near the

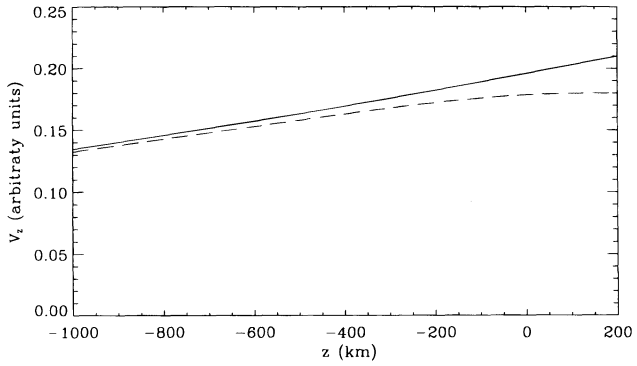

FIG. 5.—The eigenfunctions v_z as a function of z for a mode of frequency $\nu = 2$ mHz in a uniform B field ($B = 200$ G). The solid line shows the eigenfunction for the nonmagnetic model, and the dashed curve the eigenfunction in the presence of a uniform magnetic field (case 1). Note that the amplitude near the surface is suppressed in the presence of a uniform field.

surface. This is because deep down in the polytrope, the plasma β, defined as the ratio of gas pressure to magnetic pressure, is very large and hence the effect of the magnetic field on v_z is insignificant. However, near the surface one expects magnetism to play an important role since β is small. In Figure 5, we show the region near the surface. It is clear from Figure 5 that the amplitude of the eigenfunction is reduced in the presence of a uniform magnetic field.

We also consider a mode of higher frequency to see if the eigenfunctions vary by a different amount. In Figure 6, we repeat plots of Figure 5 except that we now consider $\nu = 4$ mHz. Note that the effect is larger at 4 mHz than at 2 mHz despite the fact that the change in turning point is not as large at 4 mHz as it is at 2 mHz. Inspection of Figure 6 shows that the eigenfunctions for the magnetized and unmagnetized atmospheres cross several times below the turning points, because the phases and wavelengths are slightly different (although the wavefunction at depth in the magnetized model turns out to be nearly the J function). If we could see to all depths we would see alternating enhancement and suppression of power. Another example of this occurs in the next case.

In Figure 7, we investigate the effects of greater magnetic field strength ($B = 400$ G) for the mode of frequency $\nu = 4$ mHz. It is obvious from comparing Figures 6 and 7 that all effects are larger, including the phase shifts.

In Figure 8*a*, we illustrate the eigenfunctions as a function of z for a mode of frequency 1.5 mHz in the presence of a

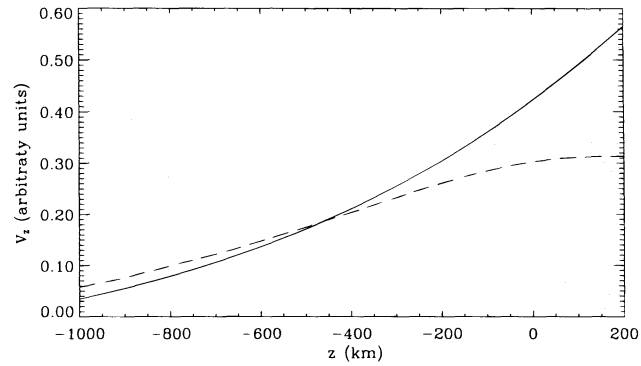

FIG. 6.—Same as Fig. 5 except that here the frequency of the mode is $\nu = 4$ mHz.

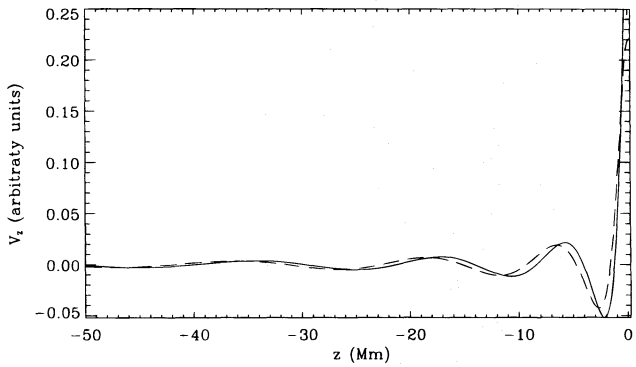

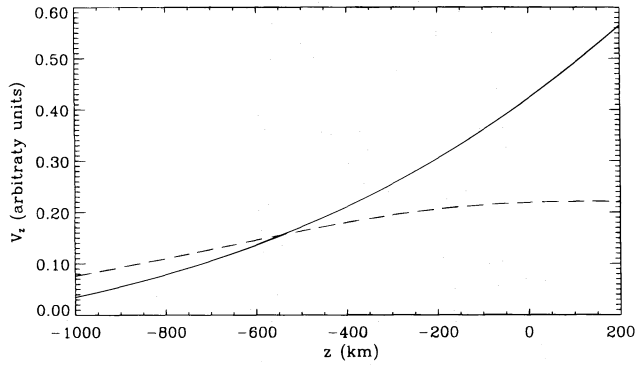

FIG. 7.—Same as Fig. 6 except that here the magnetic field strength $B = 400$ G. Note that the eigenfunctions for the magnetized and unmagnetized atmospheres cross several times below the turning points, because the phases and wavelengths are slightly different.

constant v_A field (case 2). Again, the surface amplitude in the presence of such a field is suppressed in comparison to the nonmagnetic case. In this case, since the magnetoacoustic cutoff frequency decreases compared to the nonmagnetic case (see Fig. 2), one would expect the surface amplitude to be enhanced. We plot κ^2 (see eq. [8]) as a function of z in Figure 8*b*. The dashed line corresponds to the constant v_A case and the solid line to the nonmagnetic case. It appears that the vertical wavelength increases below ≈ -1000 km in the presence of magnetism. As a result the nodes get slightly shifted toward the surface. So, even though the turning point is raised compared to the nonmagnetic case, the surface amplitude decreases because of the shift in the wavefunction.

In Figure 9, we consider a mode of frequency $\nu = 1.8$ mHz and plot the eigenfunctions as a function of z for the nonmagnetized and magnetized models (case 3). Unlike Figures 6 and 7, Figure 8 shows that the change in the amplitude of the eigenfunction in the presence of a Gaussian-type magnetic field profile is insignificant, as expected from the discussion of Figure 3*c*. Similar results are obtained for other values of ν. This is further due to the limitation of these polytropic models to large β, so that the entire atmosphere is gas pressure dominated. This is another reason which motivates us to consider case 4, in which it is now possible to have a low β regime.

Figure 10 shows the eigenfunctions for the marginally stable model (for case 4) as a function of z for a mode of frequency $\nu = 4$ mHz. It is interesting to note that the power in this case is only slightly suppressed in the presence of magnetism. We predicted this from the appearance of Figure 4*e*, which shows tall but thin magnetoacoustic bar-

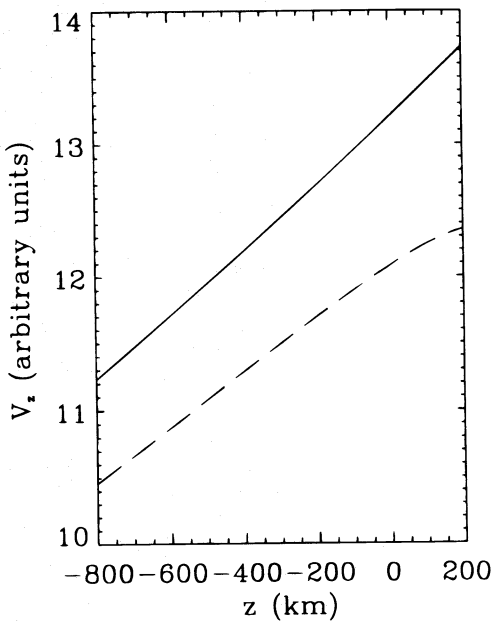

FIG. 8*a*

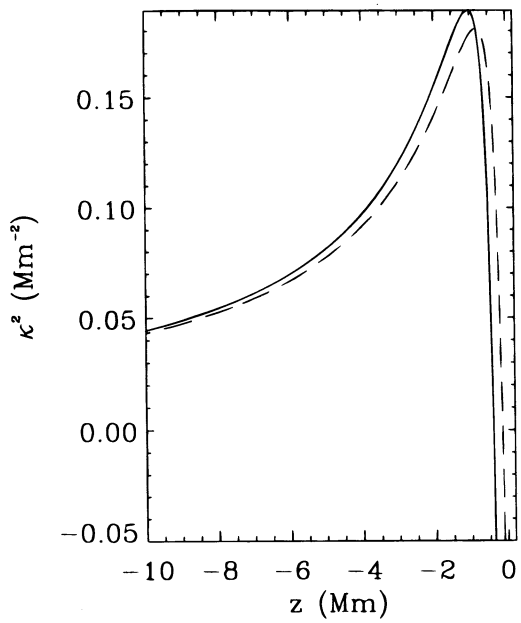

FIG. 8*b*

FIG. 8.—(*a*) The eigenfunctions v_z as a function of z. The solid line shows the curves for nonmagnetized model and the dashed curves in the presence of a constant Alfvén speed atmosphere (case 2). (*b*) The square of vertical wavenumber κ^2 as a function of z for magnetized (case 2) and nonmagnetized atmospheres.

riers at depth. It should be noted that the power measured at fixed temperature instead of a fixed geometrical height for such a model would actually show enhancement compared to the nonmagnetized case. For example, in Figure 10, $T = 6000$ K corresponds to $z \approx 0$ for magnetized and $z = -100$ km for nonmagnetized model and so if we consider power at this temperature, it will appear to be enhanced.

3.3. *Equivalence of Magnetic and Acoustic Perturbations*

In a nonmagnetic atmosphere, the acoustic cutoff frequency is given by equation (10). Imagine a small acoustic perturbation $\Delta c_s^2(z)$ in c_s^2. Linearizing in $(\Delta c_s^2/c_s^2)$ gives a correction to ω_{ac}^2 which can be written as

$$\Delta\omega_{ac}^2 = -\omega_{ac}^2 \frac{\Delta c_s^2}{c_s^2} + \frac{\gamma g}{2c_s^2}\frac{d\Delta c_s^2}{dz}. \tag{23}$$

In a magnetic atmosphere, the magnetoacoustic cutoff frequency is given by equation (9). Assuming $(v_A^2/c_s^2) \ll 1$ we linearize and obtain a correction to the magnetoacoustic cutoff frequency, $\Delta\omega_{mac}^2$,

$$\Delta\omega_{mac}^2 = -\omega_{ac}^2\left(\frac{v_A^2}{c_s^2}\right) + \frac{(2-\gamma)\gamma g v_A^2}{2c_s^2 H_m} + \frac{(2-\gamma)v_A^2}{2c_s^2 H_m} \times \frac{dc_s^2}{dz} - \frac{(2-\gamma)}{2}\frac{d}{dz}\left(\frac{v_A^2}{H_m}\right) + \frac{\gamma g}{2c_s^2}\frac{dv_A^2}{dz}. \tag{24}$$

Note that if γ were equal to 2, $\Delta\omega_{mac}^2$ would be equal to $\Delta\omega_{ac}^2$ if we just set $v_A^2 = \Delta c_s^2$. However, since the compressibility of

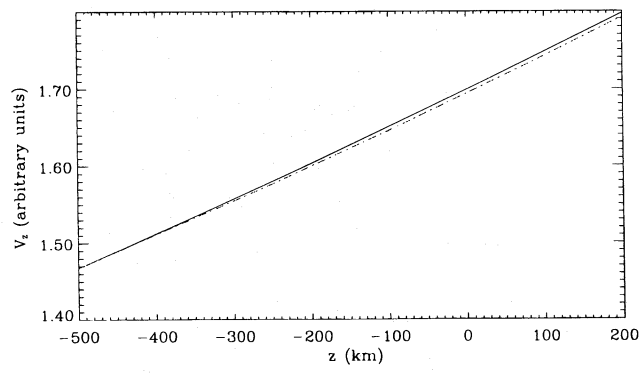

FIG. 9.—The eigenfunctions v_z as a function of z. The solid line shows the curves for the nonmagnetized model, and the dot-dashed curve shows the presence of a Gaussian-type magnetic field (case 3).

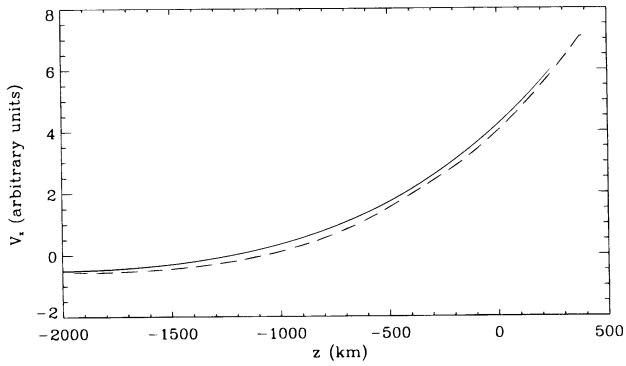

FIG. 10.—The eigenfunctions v_z as a function of z for a mode of frequency $\nu = 4$ mHz. The solid line shows the curves for nonmagnetized model and the dashed curves for a neutrally stable model with localized magnetic field (case 4). The field strength at $z = -300$ km corresponds to ~415 G. Note that the power in this case is only slightly suppressed. However, if the power is measured at a fixed temperature instead of a fixed geometrical height for such a model it would actually show enhancment compared to the nonmagnetized case. For example, $T = 6000$ K corresponds to $z \approx 0$ for magnetized and $z \approx -100$ km for nonmagnetized model, and so if we consider power at this temperature, it will appear to be enhanced.

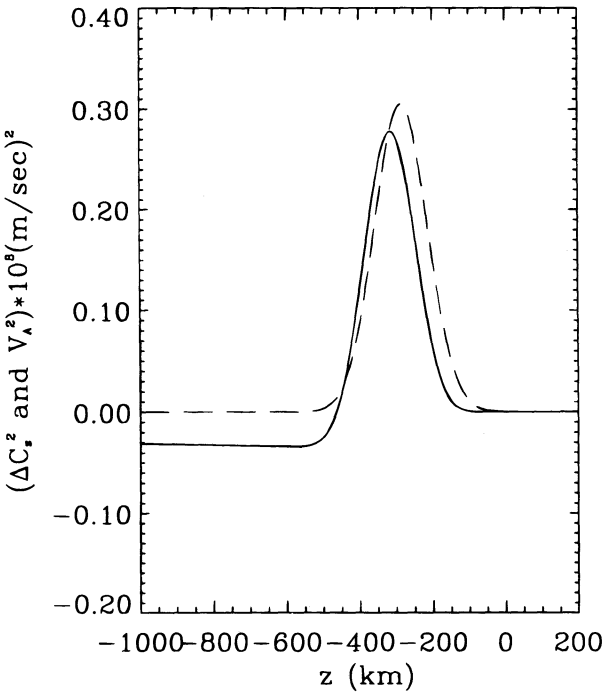

FIG. 11.—The square of perturbed sound speed (*solid line*) and the Alfvén speed (*dashed line*) as a function of z for the Gaussian profile field (case 3).

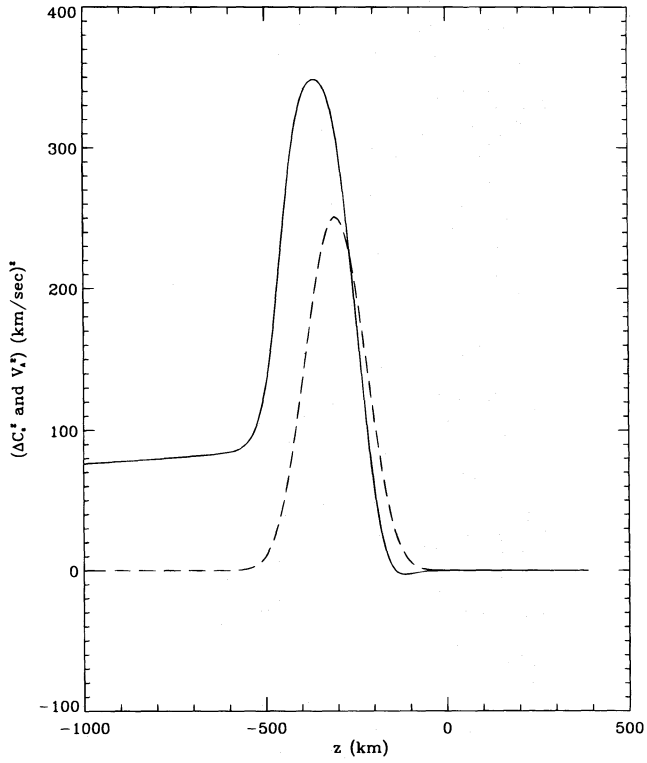

FIG. 13.—The square of perturbed sound speed (*solid line*) and the Alfvén speed (*dashed line*) as a function of z for marginally stable model (case 4). As can be seen from eq. (26), the sound speed never returns to its unmagnetized value, although the relative perturbation becomes smaller with depth.

the thermal and magnetic gas are different ($\gamma \neq 2$), the two types of perturbation cannot be exactly the same. Let us treat the magnetic field as known and solve for the acoustic profile that gives the same turning point perturbation by equating (23) and (24):

$$\frac{\gamma g}{2c_s^2}\frac{d}{dz}\Delta c_s^2 - \frac{\omega_{ac}^2}{c_s^2}\Delta c_s^2 = \frac{\gamma g}{2c_s^2}\frac{dv_A^2}{dz} - \frac{\omega_{ac}^2}{c_s^2}v_A^2 + \frac{(2-\gamma)}{2} \times \left(\frac{\gamma g v_A^2}{c_s^2 H_m} + \frac{v_A^2}{H_m c_s^2}\frac{dc_s^2}{dz} - \frac{d}{dz}\frac{v_A^2}{H_m}\right) \equiv \frac{\gamma g}{2c_s^2}F(z)\,. \quad (25)$$

Equation (25) is a first-order ordinary differential equation (ODE) for $\Delta c_s^2(z)$. The solution is

$$\Delta c_s^2(z) = \int_{z_c}^{z} du F(u) \exp\left[\int_u^z dw \frac{2\omega_{ac}^2(w)}{\gamma g}\right], \quad (26)$$

which satisfies the boundary condition $\Delta c_s^2(z_c) = 0$. In some cases one might let $z_c \to -\infty$ on the grounds that it is difficult to produce thermal perturbations at depth. In the case of a buried magnetic field with β becoming large both near the surface and at depth, equation (26) shows that Δc_s^2 cannot vanish both near the surface and at depth, but must take on a constant value at one of these locations.

It is interesting to note that for a uniform field (case 1), all the terms inside the large parentheses on the right-hand side of equation (25) are zero, yielding $\Delta c_s^2 = v_A^2$ (neglecting the homogeneous solution). This was expected from comparing the expressions of acoustic cutoff frequencies (see eqs. [9] and [10]) between a uniform B atmosphere and a nonmagnetic atmosphere. Thus, in the presence of a uniform

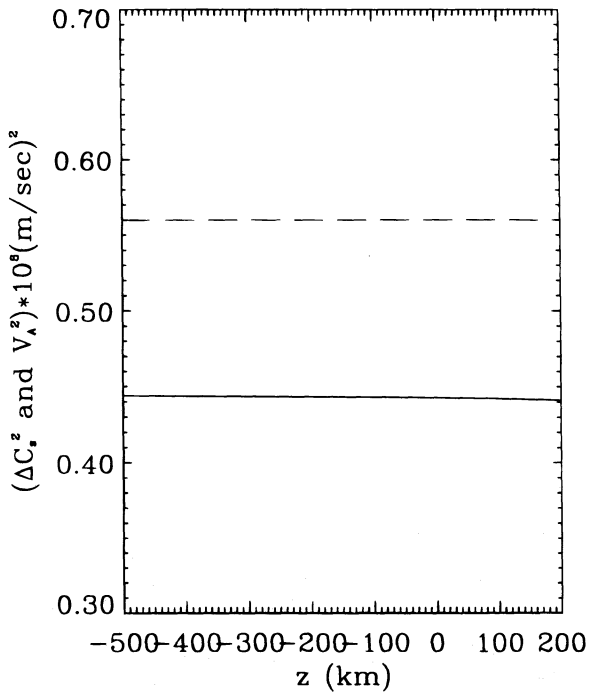

FIG. 12.—The square of perturbed sound speed (*solid line*) and the Alfvén speed (*dashed line*) as a function of z for the uniform v_A model (case 2).

field, even if the compressibility of the thermal and magnetic gas are not the same ($\gamma \neq 2$), a perturbation in the acoustic cutoff frequency can be produced by any model with the same fast mode speed.

For the Gaussian profile (case 3), the condition $(v_A^2/c_s^2) \ll 1$ is valid except right at the surface. So we solve equation (25). The homogeneous solution is given by $\Delta c_s^2 = [\alpha(z_0 - z)^{-(m-1)/2}]$ where α is an arbitrary constant of integration. We find a particular solution to equation (25) by numerically integrating from depth to the surface, which in general will not satisfy the boundary condition of a finite Δc_s^2 at the surface. We then add the homogeneous solution to this particular solution. This allows Δc_s^2 to be finite at the surface. We plot Δc_s^2 and v_A^2 as a function of z in Figure 11.

When the constant v_A case is considered (case 2), the inequality $v_A^2/c_s^2 \ll 1$ is satisfied only below -300 km, so equation (25) is invalid. However, we can proceed by equating (9) and (10) and solving for the perturbed sound speed, c_{sp}, from the following resultant equation:

$$\frac{dc_{sp}^2}{dz} = \frac{2c_{sp}^2}{\gamma g}\,\omega_{mac}^2 - \frac{\gamma g}{2}\,. \tag{27}$$

In Figure 12, we plot $(c_{sp}^2 - c_s^2)$ and v_A^2 as a function of z. Recall that v_A is uniform and is ~ 7.5 km s^{-1} throughout the polytrope.

For the neutrally stable atmosphere with localized field (case 4), we once again solve equation (27) but now from the new surface $z = z_s$. Since $\omega_{mac}^2 \rightarrow [\gamma g(m+1)]/[4(z_s - z)]$ near the surface, we integrate equation (27) from the surface downward considering $c_{sp}^2 \approx c_s^2$ near the surface. Figure 13 shows $(c_{sp}^2 - c_s^2)$ and v_A^2 as a function of z. As can be seen from equation (26), the sound speed never returns to its unmagnetized value, although the relative perturbation becomes smaller with depth.

4. DISCUSSION

In this paper we have used four simple models, all based on a polytrope, to show how magnetic fields affect p-mode power observed at a fixed height. We have chosen a fiducial height and temperature of -100 km and 6000 K and surface field strengths of a few hundred Gauss. The mean field in plage regions is in the range 150–200 G (Title et al. 1992) but the rms field, which is relevant to this investigation, is larger because of the concentration of the field into flux tubes. Despite the fact that magnetogram observations detect the vertical component of the field, our models are quantitatively reasonable.

We have identified four mechanisms by which magnetic fields affect surface amplitudes. First, the turning points can be lowered. Second, the skin depth in the evanescent region can be reduced. Third, the phases and wavelengths of the eigenfunctions can be changed. Finally, the temperature structure of the atmosphere itself, and hence the regions of line formation, can be affected, as in Figures 4 and 10.

Although we have demonstrated suppression by 40%–60% in some cases (Figs. 6 and 7), the circumstances under which this occurs appear to be rather tightly constrained. Models in which the field is stored in a thin, subsurface layer show little suppression, either because the fields we constructed are small (case 3) or, more generally, because the changes are so spatially localized that the modes can tunnel through them (cases 3 and 4). The field apparently has to be strong near the surface (cases 1 and 2).

We also showed that changes to the cutoff frequency brought about by a magnetic field can also be caused by an acoustic perturbation, which can be constructed by solving a first-order ODE. However, the other propagation characteristics of the modes will differ, because the cutoff frequency and magnetoacoustic speed in the two models cannot *simultaneously* be made the same.

The analysis is based on polytropic models where the pressure and density must vanish at some height in the atmosphere. Above this height exists a vacuun. The wavefunctions in such models can be strongly affected by the surface boundary condition. Modes of 3 or 4 mHz have an upper turning point that is less than a skin depth from the surface. Another problem is that the Alfvén speed becomes infinite at the surface, which greatly modifies the surface boundary condition. It is also worth noting that since we have not developed a thermodynamically self-consistent solar model, the presence of a magnetic field alters the density and temperature structure in a manner that we can prescribe somewhat arbitrarily. However, Hindman (1995) has developed a self-consistent solar model where the solar interior smoothly matches onto an outer atmosphere. He also finds that the field must be strong near the surface to achieve suppression. Evans & Roberts (1990) have also found that for $k \neq 0$ the surface amplitudes reduce in the presence of a uniform field embedded in an isothermal atmosphere.

We now briefly mention the ramifications of our results for two other helioseismic diagnostics: wave travel times, and wave phase shifts.

Because of the lowering of the upper turning point and the increase in the progagation speed of the wave in the presence of magnetic fields, we expect the wave travel time between one location and another in the active and quiet regions to be different (see Jefferies et al. 1994; Duvall et al. 1995). We will address this issue in some detail in our future work but on the basis of this analysis, we expect the wave travel time in the magnetic region (for example, where the upper turning point is lowered by ~ 300 km) to be shorter by as much as 30 s.

Direct examination of equation (6) suggests that the presence of magnetism affects the vertical wavenumber κ through the acoustic cutoff frequency and the propagation speed. This in turn changes the vertical wavelength and the phase of the p-modes. The comparison between phase differences measured at a given height between the modes propagating in active regions and a weakly magnetized nearby regions may well give some information about the magnetic field structure in active regions. We strongly recommend simultaneous *phase* observation of the p-modes in active and quiet regions of the Sun.

The present investigation is for $k \rightarrow 0$, but it suggests that a comparison of p-mode power between quiet and active regions would vary as a function of frequency and horizontal wavenumber.

Finally, although we did not perform a modal calculation, our work has bearing on the *frequencies* of p-modes that are affected by magnetic fields (Campbell & Roberts 1989; Evans & Roberts 1990; Goldreich et al. 1991; Jain & Roberts 1993). The field strength varies with time and with location as active regions merge and decay on the solar surface. On a longer timescale, variations with the solar cycle are also to be expected (Bachmann & Brown 1993). On the basis of this analysis, we expect changes in the size of

the p-mode cavity and the rate at which the eigenfunctions decay in the evanescent region. All these would be reflected in the frequency shifts and linewidths of the p-modes.

The general conclusion to be drawn is that the upper turning point changes due to magnetism and that observations at different heights in the evanescent tail of the eigenfunction will yield different power in the solar p-modes when compared between the magnetic and nonmagnetic (or weakly magnetized) regions.

We appreciate financial support from NASA through the Solar Oscillations Investigation, the Space Physics Theory Program, and the Graduate Student Research Program, and from the NSF through Grant AST 95-21779. We are also happy to acknowledge useful discussions with T. Brown, T. Duvall, Jr., D. Gough, and B. Roberts.

REFERENCES

Abramowitz, M., & Stegun, I. A. 1970, Handbook of Mathematical Functions (New York: Dover)
Bachmann, K. T., & Brown, T. M. 1993, ApJ, 411, L45
Bogdan, T. J., & Zweibel, E. G. 1985, ApJ, 298, 867
Brown, T. 1994, GONG 1994 poster presentation, Univ. of Southern California, LA, 1994, May 16–20
Cally, P. S. 1995, ApJ, 451, 372
Campbell, W. R., & Roberts, B. 1989, ApJ, 338, 538
Duvall, T. L., D'Silva, S., Jefferies, S. M., Harvey, J. W., & Schou, J. 1995, Nature, 379, 235
Evans, D. J., & Roberts, B. 1990, ApJ, 356, 704
Gingerich, O., Noyes, R. W., Kalkofen, W., & Cuny, Y. 1971, Sol. Phys., 18, 347
Goldreich, P., Murray, N., Willette, G., & Kumar, P. 1991, ApJ, 370, 752
Gough, D. O. 1991, Astrophysical Fluid Dynamics, Les Houches XLVII, 1987, ed. J. P. Zahn & J. Zinn-Justin (Amsterdam: North Holland), 399
Hindman, B. W. 1995, Ph.D. thesis, Univ. of Colorado
Hindman, B. W., Jain, R., & Zweibel, E. G. 1966, in preparation
Jain, R., Hindman, B. W., & Zweibel, E. G. 1995, in Proc. 4th SOHO Meeting on Helioseismology, SP-376, Vol. 2, 63
Jain, R., & Roberts, B. 1993, ApJ, 414, 898
Jefferies, S. M., Osaki, Y., Shibahashi, H., Duvall, Jr., T. L., Harvey, J. W., & Pomerantz, M. A. 1994, ApJ, 434, 795
Lites, B. W., White, O. R., & Packman, D. 1982, ApJ, 253, 386
Newcomb, W. A. 1961, Phys. Fluids, 4, 391
Tarbell, T., Peri, M., Frank, Z., Shine, R., & Title, A. 1988, in Seismology of the Sun and Sun-like stars, ESA SP-286, 315
Thomas, J. H. 1983, Annu. Rev. Fluid Mech., 15, 321
Title, A. M., Topka, K. P., Tarbell, T. D., Schmidt, W., Balke, C., & Scharmer, G. 1992, ApJ, 393, 782